SELF-CONSISTENT, QUASI-3D SIMULATION OF QUANTUM WAVEGUIDE COUPLERS

A. Galick*, M. Macucci†, U. Ravaioli* and T. Kerkhoven‡
* *Beckman Institute, University of Illinois*
405 N. Mathews, Urbana, Illinois 61801
†*Dipartimento di Ingegneria dell'Informazione*
Università degli Studi di Pisa
Via Diotisalvi, 2, I-56126 Pisa, Italy
‡*Department of Computer Science, University of Illinois*
Urbana, Illinois 61801

Abstract

A quasi 3D simulation of a quantum waveguide coupler has been performed. The Schrödinger and Poisson equations have been solved self-consistently in each of the 2D slices into which the device has been subdivided. A modified recursive Green's function algorithm is used to compute the waveguide and tunneling conductances.

I. DEVICE MODEL

We have studied a device model based on the structure reported by Eugster *et al.* in Ref. 1, assuming a layer arrangement (Fig. 1) for the shallow heterostructure as reported in Ref. 2. The gate geometry of our model corresponds faithfully to the real device in the central portion, where coupling between the two waveguides takes place, while differs in the outer regions (dashed lines in Fig. 2), where we have assumed semiinfinite quantum wires instead of tapering off from a 2DEG, for reasons of computational convenience. The model has been divided into 2D slices along the longitudinal direction, assuming that the potential profile is going to be constant within each slice. The Schrödinger and Poisson equations have been solved self-consistently in each slice, obtaining eigenvalues and eigenfunctions to be used for the conductance calculation. Our quasi-3D approach is based on the hypothesis of quasi-adiabatic variation of the potential along the longitudinal direction, which allows solving for the potential separately in each slice. Finally, the Green's functions for the whole structure are computed and from them we obtain the transmission coefficients and, consequently, the conductances, via the Landauer formula.

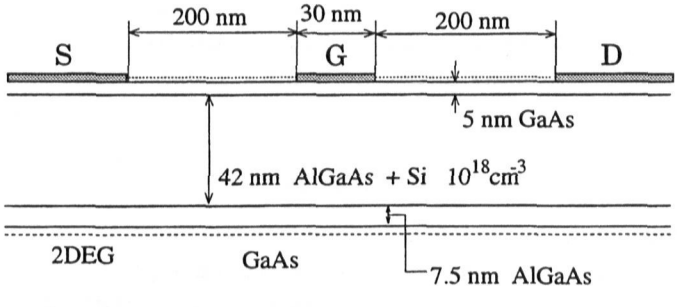

Fig. 1. Layer diagram of the heterostructure

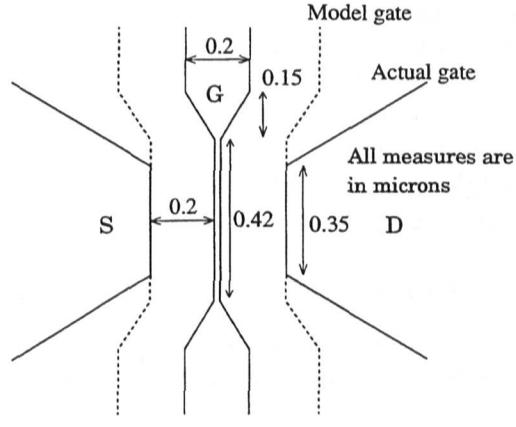

Fig. 2. Gate geometry

II. MODIFIED GREEN'S FUNCTION METHOD

In order to compute the transmission and reflection coefficients and thus the conductances in our model device, we have used a modified version [3] of the Recursive Green's Function Formalism [4,5,6].

The basic idea consists in computing the Green's functions for 1D chains with Dirichlet boundary conditions at their ends. Each 1D chain represents the propagation of a 2D transverse mode within a slice characterized by a constant transverse potential profile. Due to the invariance of the potential along the longitudinal direction, the various transverse modes do not couple within a single slice, therefore their representation with 1D chains is rigorously correct.

The Dirichlet boundary conditions imply isolation of each section from the neighboring ones. The Green's functions of the connected structure are evaluated by applying a perturbation corresponding to joining the ends of the chains belonging to different sections and removing the Dirichlet boundary conditions. The perturbed Green's functions are obtained from the Dyson equation, evaluating the effect of the perturbation to all orders

$$G = G_0 + G_0 \hat{V} G,$$

where G_0 is the Green's function for the unperturbed system, G the one for the perturbed system and $\hat{V}$ represents the perturbation potential, corresponding to coupling between neighboring slices.

The Green's functions for each 1D chain are computed with a discretization based on a tight-binding description of the device geometry. The present approach, however, differs from the one of Ref. 6, because we are not using a square tight-binding lattice. Usage of a square lattice is convenient when studying disorder induced phenomena, i.e. when rapid fluctuations of the potential occur in all directions. In the present calculation we use a tight-binding discretization only along the longitudinal direction parallel to the waveguides, while along the transverse direction we consider simply a number of modes sufficient to accurately describe the coupling between slices. This formulation of the problem yields an immediate advantage: it is possible to use a very fine discretization in the longitudinal direction, while keeping the number of transverse modes and therefore the size of the matrices to be inverted [6] down to reasonable values. A fine discretization in the longitudinal direction is important to obtain a good representation of the continuum energies: the actual tight-binding dispersion relation is cosinusoidal, only in the region around the origin it properly reproduces the parabolic dispersion relation of continuum.

The elements of the coupling matrix $\hat{V}$ are the mode overlaps between the transverse modes of the corresponding pair of slices, multiplied by the tight-binding hopping potential [6]. The mode overlaps are computed taking the discretized overlap integral between the wave functions relative to the modes being considered.

Numerical resolution of transverse modes in each slice requires a fine 2D grid in the quantum well (QW) region. The overlap integrals are computed on a common grid which must be fine over the QW regions of all slices and which therefore has very many lines. We use specialized methods to solve the resulting large, sparse eigenvalue problems.

III. SELF-CONSISTENT SCHRÖDINGER-POISSON SOLUTION

As in Ref. 7, the resolution of the transverse modes in each slice is an iteration to self-consistency of the Schrödinger equation for the wavefunctions and a nonlinear Poisson equation for semi-classical charges such as ionized dopants. We take the surface charge density to be constant between contacts at -3.3×10^{12} cm^{-2}. At 1.6 K, this Poisson equation is highly nonlinear, with effects such as acceptor freezeout in the substrate occurring practically discontinuously, which requires a grid refinement at the freezeout depth. The coupling between the Poisson and Schrödinger equations is also very dramatic, with slight perturbations in the potential resulting in a complete

change in the number and shape of the occupied wavefunctions. For this sensitive problem, we use a fixed-point iteration in the most sensitive quantity, the quantum electron density.

The iteration progresses by successive solution of the nonlinear Poisson and Schrödinger equations. It is clear that a fixed point of this iteration corresponds to a self-consistent solution. It is also clear that the nature of the iteration will be oscillatory, with underfull wavefunctions causing a deepening of the QW, leading to overfull wavefunctions, and vice versa. In the early iterations, we use adaptive underrelaxation to stabilize the oscillations. Close to the solution, we use a Jacobian-free approximate Newton method to accelerate the convergence to self-consistency. Our experience is that this is a very effective way to handle the nonlinearlity in the model [8].

The nonlinear Poisson equation is solved using a Newton method with inexact linesearch. We take zero-field boundary conditions in the air above the contacts and to the sides, Dirichlet boundary conditions in the contacts that include a Schottky barrier of 0.9 eV, and Dirichlet boundary conditions in the substrate for charge-neutrality, determined by a bisection search of the bandgap. The Jacobian is solved for the Newton direction using the Conjugate Gradient (CG) method on a reduced system obtained by block Gaussian elimination of a red-black reordering of the matrix from a 5-point discretization on a rectangular grid, as in [8]. This gives an order of magnitude speedup over straight CG.

The eigenvalue problem for the Schrödinger equation can be effectively solved with a version of RITZIT [9] modified to use column operations, providing the spectrum is first shifted to make the desired eigenvalues the largest in modulus. However, we have developed a more efficient Chebyshev-preconditioned Krylov subspace method. Both of these solvers are projection methods [10], which reduce the complexity of the eigenvalue problem by finding a small invariant subspace of a matrix rather than its entire spectral decomposition. Although the fine grid to resolve the transverse wavefunctions results in a large, sparse eigenvalue problem, only the few lowest energy levels that are occupied are relevant to the problem. The higher energy levels are squashed by Chebyshev preconditioning in both solvers, so that the subspace iteration in RITZIT and our Krylov subspace iteration converge specifically to the desired modes.

IV. RESULTS

We have been interested in simulating 1D-to-1D tunneling in this structure, therefore we have chosen electrode bias values tuned to obtain significant coupling between the wires. It turns out that appreciable coupling is reached only with a central gate bias of -0.6 V, which corresponds to the threshold for depletion of the 2DEG under an infinite gate. In our model device this does not lead to coupling between the outgoing leads, due to the depleting action of the source and drain electrodes that are in close proximity of the gate. In the real device geometry, at this gate voltage the two channels would probably be short-circuited, due to strong coupling far from the central region. This may be the explanation for the problems reported [11] in the observation of 1D-to-1D tunneling.

In Fig. 3 we report the results for the conductance between the ends of the same waveguide (upper curve) and between the end of one waveguide and the other end of the other waveguide (lower curve) vs. the length of the central slice, where most of the coupling takes place. Bias values are constant: V_G=−0.6 V, $V_D = V_S$=−1.65 V. As expected, we observe a substantially oscillatory behavior of the tunneling conductance for increasing length of the central section. Oscillations in the tunneling conductance have opposite phase with respect to the ones in the direct conductance in order for the total current to be constant. Even in this extreme bias condition the coupling never reaches $2e^2/h$.

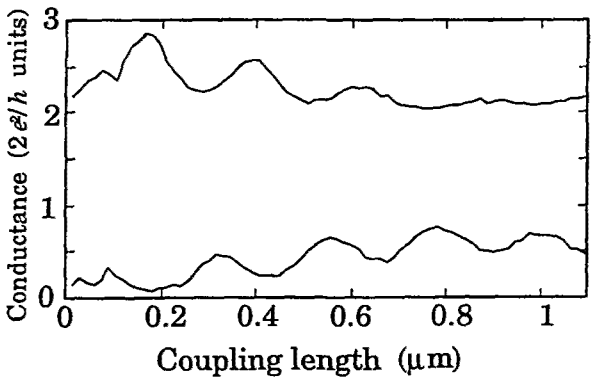

Fig. 3. Conductance between the end of the same waveguide (upper curve) and tunneling conductance (lower curve) vs. coupling length.

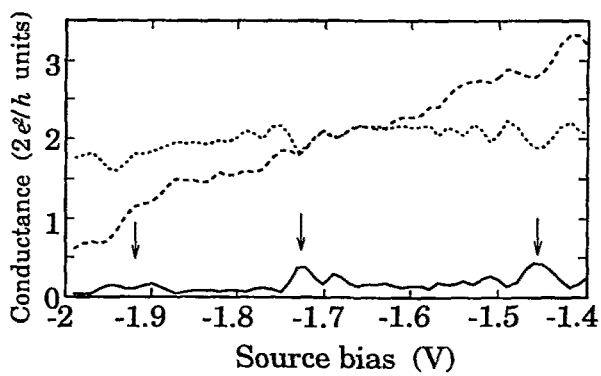

Fig. 4. Conductance of the drain waveguide (dotted line), of the source waveguide (dashed line) and tunneling conductance (solid line) vs. bias.

In Fig. 4 results are shown for the conductance of the source-side waveguide (dashed line), the drain-side waveguide (dotted line) and between the two waveguides (solid line) as a function of the bias of the source electrode. The gate and drain biases are kept constant at -0.6 V and -1.7 V, respectively. We observe peaks (indicated by arrows) of the tunneling conductance in correspondence with the opening of new modes in the source waveguide, in analogy with what has been observed experimentally for the 1D-to-2D tunneling. Conductance quantization for the source waveguide when the source bias is swept is rather poor, as in the experimental results of [1]. This may also be due to reflections in the bends, besides the effects of finite temperature (1.6 K) and of coupling.

ACKNOWLEDGMENTS

This work has been supported through the NSF grant ECS 91–20641. One of the authors (M. M.) acknowledges also support from the CNR (Italian National Research Council).

REFERENCES

[1] C. C. Eugster and J. A. del Alamo, Phys. Rev. Lett. **67**, 3586 (1991).

[2] M. J. Rooks, C. C. Eugster, J. A. del Alamo, G. L. Snider and E. L. Hu, J. Vac. Sci. Technol. B **9**, 2856 (1991).

[3] M. Macucci, U. Ravaioli and T. Kerkhoven, Superlattices and Microstructures **12**, 509 (1992).

[4] D. J. Thouless and S. Kirkpatrick, J. Phys. C **14**, 235 (1981).

[5] F. Guinea and J. A. Vergés, Phys. Rev. B **35**, 979 (1987).

[6] F. Sols, M. Macucci, U. Ravaioli, and Karl Hess, J. Appl. Phys. **66**, 3892 (1989).

[7] S. E. Laux and F. Stern, Appl. Phys. Lett. **49**, 91 (1986).

[8] T. Kerkhoven, A. Galick, U. Ravaioli, J. Arends, and Y. Saad, J. Appl. Phys. **68**, 3461 (1990).

[9] H. Rutishauser, Numer. Math. **16**, 205 (1970).

[10] Y.Saad, in Matrix Pencils, Proceedings, P. Havsbad, B. Kagstrom and A. Ruhe, Eds., 121 (1982).

[11] J. A. del Alamo, private communication